Hindawi
Advances in Materials Science and Engineering
Volume 2024, Article ID 2494900, 9 pages
https://doi.org/10.1155/2024/2494900

Research Article

Influence of Tool Pin Profiles on Aluminium Alloy A356 and Ceramic-Based Nanocomposites for Light Weight Structures by Friction Stir Processing

L. Karthick,[1] Mruthunjaya M.,[2] Srinivas. S.,[3] Prasanna Venkatesh R.,[4] Naveen Kumar Gurajala,[5] Meghavath Mothilal,[6] and Hari Banda[7]

[1]*Department of Mechanical Engineering, Hindusthan College of Engineering and Technology, Coimbatore 641032, India*
[2]*Department of Mechanical Engineering, JSS Academy of Technical Education, Dr. Vishnuvardhan Road, Bengaluru 560060, India*
[3]*School of Mechanical Engineering, REVA University, Rukmini Knowledge Park, Kattigenahalli, Yelahanka, Bengaluru 560064, India*
[4]*Department of Mechanical Engineering, SACS MAVMM Engineering College, Madurai 625301, India*
[5]*Department of Mechanical Engineering, CMR College of Engineering and Technology, Hyderabad 501401, Telangana, India*
[6]*School of Mechanical Engineering, Vellore Institute of Technology, Katpadi, Vellore, Tamil Nadu-632014, India*
[7]*Department of Mechanical Engineering, Villa College, Boduthakurufaanu Magu, Maldives*

Correspondence should be addressed to L. Karthick; bemechkarthick@gmail.com and Hari Banda; banda.hari@villacollege.edu.mv

Received 22 October 2022; Revised 14 February 2023; Accepted 16 November 2023; Published 18 March 2024

Academic Editor: P. M. Gopal

In this research, the main aim is to focus the enhancement of aluminium-based metal matrix composites for improving the attributes of light weight metals, aerospace structures and other tailor blank material properties. By this way, the friction stir processing (FSP) was the suited alternate technique to enhancing the mechanical attributes and superior microstructural amendment in the processed MMCs. Therefore, this study investigates the dispersion of ceramic-based strengthening particles of chromium oxide (Cr_2O_3) in the aluminium base matrix of A356 alloy. During the processing, the different tool pin sizes having the conical threaded tool pin profiles. Similarly, the tool spinning speed and tool travel speed also varied while in FSP. Before the processing, the A356 alloy was prepared by the grooved surfaces for packing the chromium oxide particles to compose the aluminium metal matrix composites. The tensile strength and hardness was employed to carry out from the friction stir processed A356 alloy with influencing of Cr_2O_3. The maximum occurred tensile processing parameters are 1500 rpm of spinning speed, 6 mm of tool pin sizes and 90 mm/min of tool travel speed. Similarly, the maximum obtained hardness processing parameter are 2000 rpm of spinning speed, 5 mm of tool pin sizes and 90 mm/min of tool travel speed. A scanning electron microscope was utilized to investigate the dispersed Cr_2O_3 in the A356 alloy for confirming the refinement grains in the nugget zones of FSPed A356 alloy. The increased grain boundary by the influence of different tool pin sizes was the major reason to produces the better mechanical properties in the processed A356/Cr_2O_3.

1. Introduction

In various engineering industries such as aerospace, automobile, and other light weight-related manufacturing applications, aluminium plays the major role to produce the light weight structures by the utilization of various processing technologies [1–5]. Normally, the aluminium alloys had better mechanical attributes due to their enhanced corrosion, recyclability, low weight, and alleviate to formability. In the normal aluminium alloys, the mechanical

strength and its wear performances are improved minimally when the reinforcements were not added up together. While in the process of fabrication in the lightweight materials, reinforcement is very captious role for improving the mechanical attributes and also the wear properties [6–10].

Right now, the aluminium-based metal matrix composites with strengthened particles are extensively utilized in the aerospace and defense related applications in the assembly unit due to their reinforcement particles which assisted to advances in strengthening. During the processing of liquefying and other casting methods, AMCs with their ceramic-based tools have lesser toughness and ductile strength owing to weaken wettability in the composed interfaces composites [11–14]. While in the process of AMCs with their ceramic products, other major disputes like uneven homogeneous dispersion and porosity defects among the ceramic reinforcements and aluminium alloy are generated. It has been accredited that the transforms in mutually the character of strengthening particles and fabrication process will be advantageous to attaining the AMCs with enhanced attributes [15–19].

The following materials like molybdenum, tungsten, vanadium, stainless steel, aluminium nitride, and aluminium-based titanium are the materials which successfully composed the aluminium metal matrix composites by the supporting ceramic reinforcement particles. Due to the wettability, disputes are easily resolved from the different researchers. The above challenging disputes are easily resolved by the friction stir processing, because this process is totally differed from the usual friction stir welding process [20, 21]. The FSP produces the evenly dispersed particles of the reinforcement in the base matrix of aluminium alloy and also resolves the major complicated wettability issues [22–24].

The modifying the tool sizes and shapes of the FSP tool are acknowledged as the most significant technique of justifying the fabrication issues like smaller and larger sized pores in the processed metals. Different pin sizes of the FSP tool on the aluminium alloy with ceramic based composites was indicated by the various researchers. It was confirmed that the different pin having cylindrical threads caused in the better microstructure variations in the expressions of evenly dispersed particles and better grain reducing while the process of FSP [25–27]. At the same time diminishes the maximum angle boundaries of grain and produces the uninterrupted dynamic recrystallization in the welded region statements was reported by the various researchers [28–30].

To enhance the extent of blended materials and the mechanical properties are achieved maximum when utilizing the different sized FSP tools. It was exposed that the different tool pin sized with cylindrical profiles enhances the grain development in the reduction of sizes, mechanical attributes and hardness owing to considerable materials blending. From the literature, different tool pin profile sizes are the novel method to establish the intermetallic particles in the processed aluminium metal matrix composites by the FSP process [31]. On the basis of maximum speed, the joint efficiency of the AA2024-T3 plates was examined [32]. Analyses were done on the effects of nano-/micro-TiO2 on several composites, including glass and kenaf [33]. Using mechanical tests, the volume percentage of glass and banana fibre was estimated [34]. Finite element analysis was used to evaluate the AISI 4130, EN8 forged steel composite materials and estimate the stress fluctuations [35, 36].

The prominent research gaps like the effect of different sized tool pin profiles on the mechanical attributes, microstructure evolution, wear properties and corrosion behaviors performances are fulfilled by the ceramic based particles which are strengthened by the aluminium alloy in the composites processing. But it has weakened the tribo mechanical properties. Now the aluminium alloy A356 is the suitable material for replacing the 6061 aluminium alloy and this material broadly used in the truck chassis, impellers, nuclear energy implementation, aircraft structures and maximum velocity boilers.

Therefore this research is aimed to investigate the mechanical properties and microstructure examinations on the A356 aluminium alloy by the presences of ceramic particles on the V grooved surfaces of the A356 through the different pin sized threaded cylindrical FSP tool pin profiles. In this research, all the processing is produced by the friction stir processing technique with various sized threaded pin shape tool. Similarly, the microstructure and mechanical properties are majorly investigated on the FSPed A356 aluminium alloy.

2. Experimentation

In this experiments, the aluminium alloy A356 was chosen as the base matrix for composing the aluminium metal matrix composites. During the process, the A356 having the sizes of 150 mm of length, 150 mm of width and 10 mm of thickness plate was utilized and ceramic based chromium oxide nano powders having the size of 80 nm was utilized as the strengthening particles in the FSP process. The chemical composition of A356 aluminium alloy is 0.1 of manganese, 0.35 of magnesium, 0.2 of iron, 7 of silicon, 0.2 of copper, 0.1 of zinc and remaining 92.05 of aluminium, respectively. The properties of chromium oxide particles are 197°C of melting point, 99.99 g/mol of molar mass and 2.7 g/cm^3 of density, respectively. Before conducting the process of FSP, the base plate of A356 was engaged to prepare the grooves having the sizes of 3.5 mm of depth and 0.75 mm of width throughout the A356 plates. The arranged grooves were occupied by the Cr_2O_3 particles by manually. The tool material is the significant one for composing the better FSP specimen. In this research, after created the grooved surfaces on the A356 alloy, the chromium oxide particles are packed manually and then pin less tool was packing the particles without any splitting out the reinforcements during the FSP initiation. Then the onion ring structure was formed on the A356 alloy [33].

Figure 1 shows the configuration of preparing the ceramic based nano particles on the A356 aluminium alloy with grooved surfaces. In this experimentation, the appropriated tool material of high carbon high chromium steel material was the tool material to generating the different tool

pin profiles [6]. The different tool pin sizes like 4, 5 and 6 diameter of tool pin sizes with conical threaded cylindrical shapes tool was utilized for secondary process of the FSP with different processing conditions. During the FSP, tool rotational speed, cross speed and axial forces are significant processing parameters of FSP. Now in this experimentation, as per the standard literature, 90 to 110 mm/min of cross or traverse speed and various tool spinning speed from 1000 to 2000 rpm, respectively. In this research, after processed specimen of A356, samples were subjected to conduct the microstructure analysis and some necessary actions like barkers reagent was takes place on the processed samples under the 150 V with holding time of 150 seconds. Then, the etched samples are taken for the SEM analysis. The mechanical performances test like microhardness and tensile experiments was conducted on the processed A356 alloy. During the microhardness test, the processed regions like stirred region, thermomechaically affected zone, heat affected zone and unprocessed A356 alloy was location for analyzing the hardness studies. As per the ASTM E8 standards tensile specimen was prepared for conducting the tensile tests. The UTM machine with model of Instron with 1 mm/min of displacement rate was maintained for all the specimens. In this FSP preparation study, tool spinning speed is increased from 1000 to 2000 rpm, different tool pin sizes like 4 to 6 mm of conical cylinder threaded profiles and various tool travel speed from 90 to 110 mm/min, respectively. From these levels of processing parameters, Taguchi L9 was suitable for designing the parameters for conducting the friction stir processing [37, 38]. Tables 1 and 2 show the three level of processing constraints for FSP and its detailed levels, respectively. Figure 2 displays the experimentation details by the graphical view.

3. Results and Discussion

From the detailed array of L9 parameters table, all the processing constraints are conducted on the A356 alloy through the friction stir processing. Table 3 shows the overall Taguchi table for FSP processing with their outputs of tensile values and micro hardness strength values. The packed ceramic particles are well dispersed in the stirred region from the entire processing parameters. As per the detailed level of L9 Taguchi, the entire specimen was prepared by the FSP conditions. From Table 3, overall hardness and tensile was easily revealed that the increasing of spinning speed with medium level of tool pin sizes and decreasing of too travel speed achieves the better mechanical attributes than the other level processing factors. The minimum and maximum of tool pin sized FSP tool did not dispersed the ceramic particles evenly during the FSP, by this way this major reason for diminishing the hardness on the stirred areas on the A356 alloy. But the increment of tool spinning speed and reduced tool travel speed produces the finer with evenly dispersed Cr_2O_3 in the grooved surfaces of the A356 alloy. While in the medium of tool spinning speed and reduced tool travel speed with moderate sized tool pin sizes obstructing the migrating for the grain boundaries. Therefore, the hardness load and superior hardness was

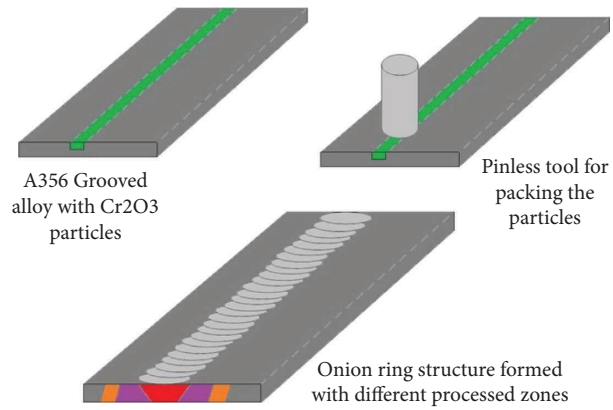

Figure 1: Configuration of grooving surfaces on the A356 aluminium alloy.

Table 1: Taguchi three level FSP constraints.

S.No.	Processing constraints	Initial levels	1	2	3
1	Tool spinning speed (rpm)	SS	1000	1500	2000
2	Tool pin sizes	TPS	4	5	6
3	Tool travel speed (mm/min)	TTS	90	100	110

Table 2: The FSP constraints with L9 method.

S.No.	SS (rpm)	TPS (mm)	TTS (mm/min)
1	1000	4	90
2	1000	5	100
3	1000	6	110
4	1500	4	100
5	1500	5	110
6	1500	6	90
7	2000	4	110
8	2000	5	90
9	2000	6	100

accumulated against hindered migration of the dislodgment during the tests. According hall Petch relationship, above the enhanced hardness values is confirmed. At the same time, stirred zones provides the refined grains and also defended from thermal heat input and also this is the confirmations for producing the maximum hardness in the particular stirred zones. In the dislodgment density of the refined grain structure area, there is an essential betterment in that dislodgment which also confirmed from the Orowan strengthening mechanism by the confirmation. From the various nine processing parameters, all the processing parameters achieved better tensile properties than the unprocessed base materials. The greater maximum spinning speed of the tool, lesser tool travel speed and medium of tool pin sizes composes the maximum tensile strength on the processed regions of A356 alloy. The maximum greater efficient of fine grain structure composes the excellent grain boundaries in the stirred regions and then enhanced grain boundaries produces the maximum obstruct to dislodging transferring of particles which is openly superior to the

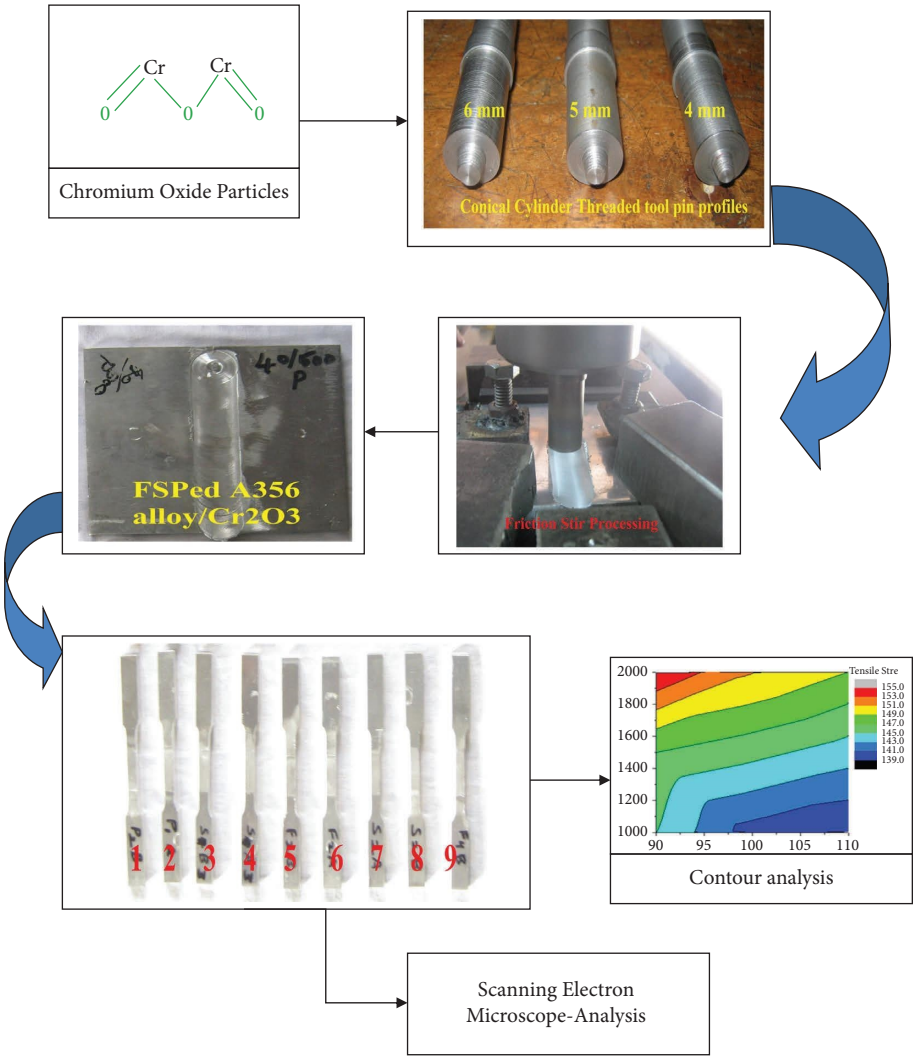

Figure 2: The experimentation details for FSP process.

obstruct per unit length of dislodging in the processed ceramic based composites. The connected strengthening particles highly praised to protect the dislodging shifting and migrated stress from the A356 to Cr_2O_3 particles. Figures 3 and 4 shows the outputs of FSPed A356 alloy. Figure 5 shows the hardness on the various processed zones of friction stir processed A356 and Cr_2O_3.

3.1. Contour Analysis of Tensile and Hardness of Friction Stir Processed A356 and Cr_2O_3. Figures 6–8 show the contour or interaction effects of different processing of FSP parameters; like tool spinning speed, tool pin sizes and tool travel speed on the friction stir processed A356 alloy and chromium oxide strengthens particles. Figure 6 shows the tool spinning speed and tool pin sizes with conical cylindrical profiles on the attained tensile strength of A356 and chromium oxide particles by the FSP. From Figure 6, it is revealed that the increment of tool spinning speed (1500 to 2000 rpm) and medium sizes of the tool pin sizes (5 mm) shows the maximum tensile strength on the FSPed A356/chromium oxide particles. Figure 7 shows the tensile strength of processed A356 alloy with chromium oxide particles with conducting the different processing factors of tool pin sizes and tool travel speed. Form Figure 7, it is exposed that the mechanical properties are improved between the improved of tool pin sizes from 4 to 5 mm and lesser tool travel speed creates the plasticized region on the stirred zones was the major reason to improves the mechanical strength. Figure 8 exhibits the different processing parameters of FSP like tool travel speed and spinning speed on the processed A356 and chromium oxide particle through the FSP for producing the tensile properties on the stirred portions. From Figure 8, it uncovered that the maximum of tensile values are correlated between the 2000 rpm of tool spinning speed and 90 mm/min of travel speed of tool creates.

Figures 9–11 show the contour or interaction effects of remarkable processing of FSP parameters; like tool spinning speed, tool pin sizes and tool travel speed on the friction stir processed A356 alloy and chromium oxide strengthens particles. Figure 9 shows the tool spinning

Table 3: Friction stir processed A356 alloy outputs by L9.

S.No.	SS (rpm)	TPS (mm)	TTS (mm/min)	Tensile strength (MPa)	Hardness (HV)
1	1000	4	90	145	95
2	1000	5	100	140	93
3	1000	6	110	139	91
4	1500	4	100	146	100
5	1500	5	110	144	99
6	1500	6	90	147	108
7	2000	4	110	149	101
8	2000	5	90	155	105
9	2000	6	100	151	103

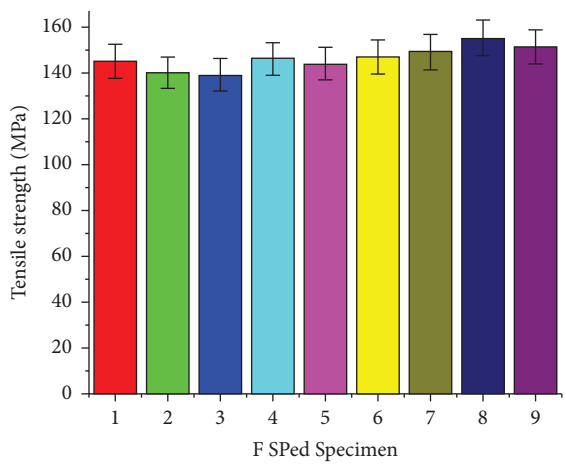

Figure 3: Tensile strength of friction stir processed Cr_2O_3 and A356 alloy.

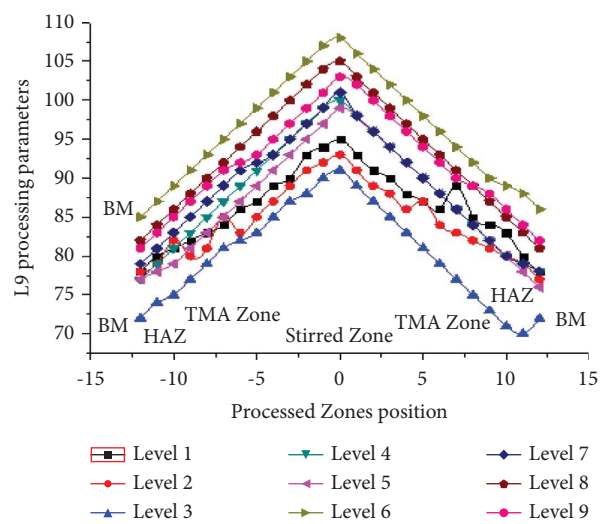

Figure 5: Detailed hardness on FSPed A356 and Cr_2O_3.

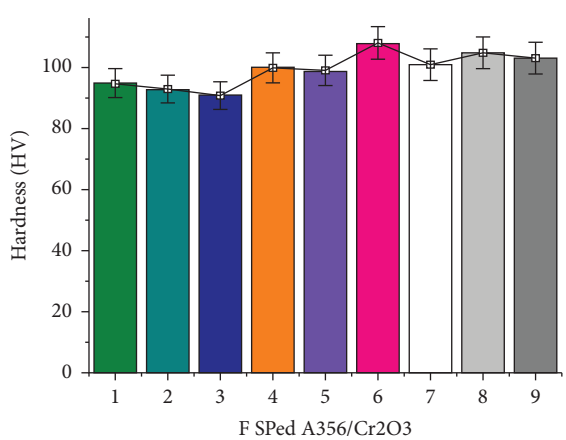

Figure 4: Hardness strength of friction stir processed Cr_2O_3 and A356 alloy.

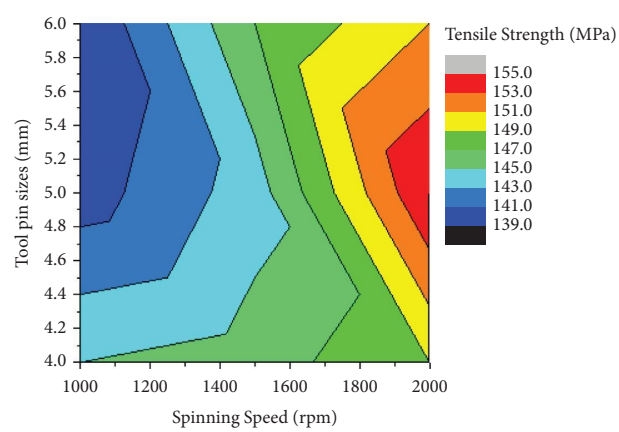

Figure 6: Spinning speed and tool pin sizes on the FSPed A356/Cr_2O_3 of tensile.

speed and tool pin sizes with conical cylindrical profiles on the accomplished hardness of A356 and chromium oxide particles by the FSP. From Figure 9, it is discovered that the increment of tool spinning speed (1500 to 2000 rpm) and maximum of the tool pin sizes (6 mm) shows the maximum hardness strength on the FSPed A356/chromium oxide particles. Figure 10 shows the hardness strength of processed A356 alloy with chromium oxide particles with performed the different processing factors of tool pin sizes and tool travel speed. Form Figure 10, it is showing that the mechanical properties are enhanced between the improved of tool pin sizes from 5 to 6 mm and minor tool travel speed generates the well plasticized region on the localized processed zones was the

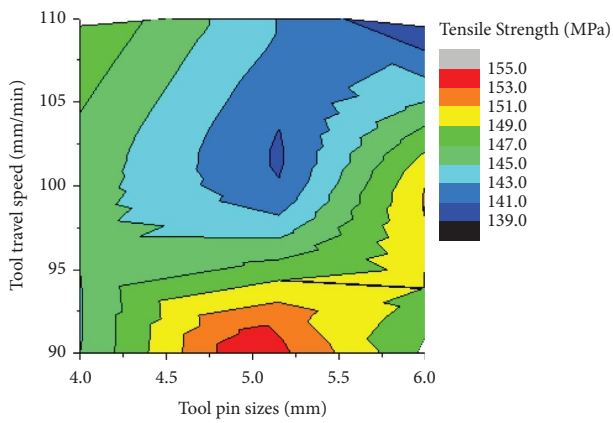

Figure 7: Tool pin sizes and tool travel speed on the FSPed A356/Cr_2O_3 of tensile.

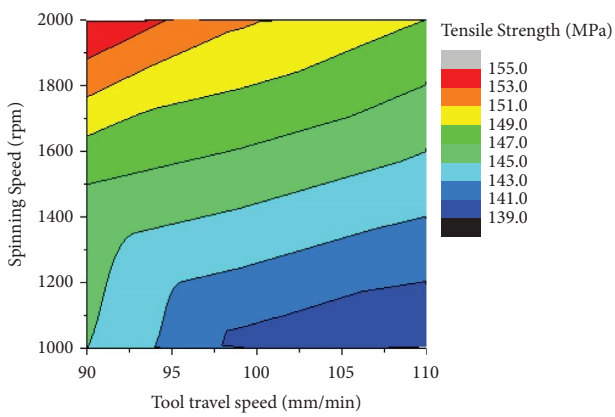

Figure 8: Tool travel speed and spinning speed on the FSPed A356/Cr_2O_3 of tensile.

main motivation to advances the mechanical potency. Figure 11 displays the various processing parameters of FSP like tool travel speed and spinning speed on the processed A356 and chromium oxide particle through the FSP for producing the hardness strength on the stirred portions. From Figure 11, it is discovered that the maximum of hardness values are correlated between the 1500 to 2000 rpm of tool spinning speed and 90 mm/min of travel speed of tool creates the consistently dispersed particles on the nugget portion of the intermetallic phases in the processed zones.

3.2. Microstructures. In this investigation, maximum of tensile and hardness attained friction stir processed samples of A356 alloy and chromium carbide particles with influences of processing parameters 1500 rpm of spinning speed, 6 mm of tool pin sizes and 90 mm/min of tool travel speed and 2000 rpm of spinning speed, 5 mm of tool pin sizes and 90 mm/min of tool travel speed, respectively, was conducted for the SEM analysis. Figures 12 and 13 show the

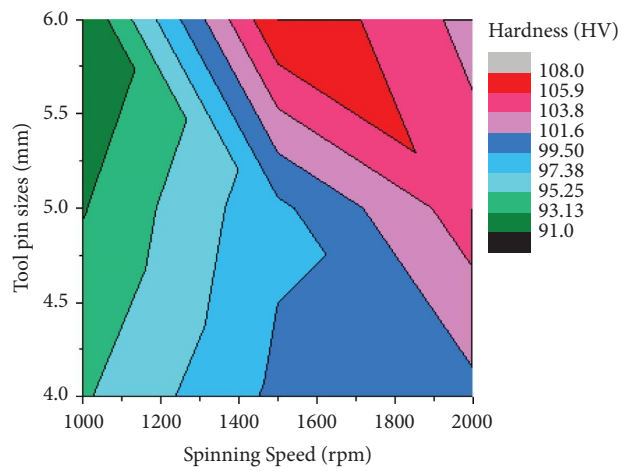

Figure 9: Spinning speed and tool pin sizes on the FSPed A356/Cr_2O_3 of hardness.

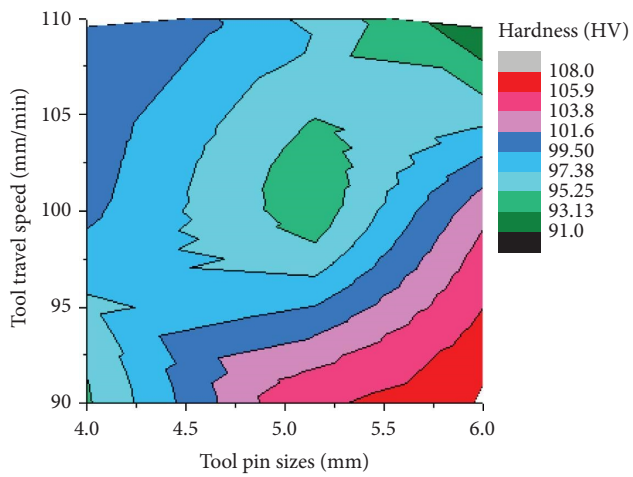

Figure 10: Tool pin sizes and tool travel speed on the FSPed A356/Cr_2O_3 of hardness.

SEM image of maximum attained specimens of tensile and hardness. Both the SEM image reveals that the surface appearances are getting finer and smoother. It is fully related to the maximized plastic deformation and sufficient material flow was accomplished by the conical threaded tool pin profiles. when compared to lower dimension of tool pin size like 4 mm, the 5 and 6 mm tool pin sizes creates the better plasticized deformation on the processed region of A356 alloy and also provides the additional shearing impact on the stirred regions. The maximum accumulation of plastic and shearing impacts was the major significant reason for enhancing the hardness and tensile strength. When increasing the tool pin sizes from 4 to 6 mm composes the better dispersed chromium oxide particles in the A356 alloy matrix and also aid to generate the greater mechanical mixing in the FSP.

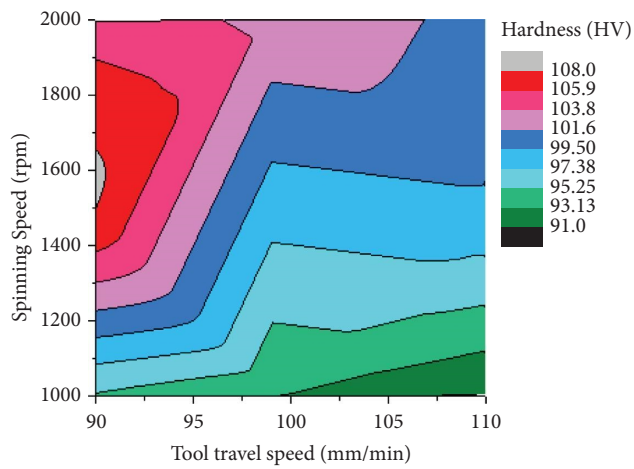

Figure 11: Tool travel speed and spinning speed on the FSPed A356/Cr_2O_3 of tensile.

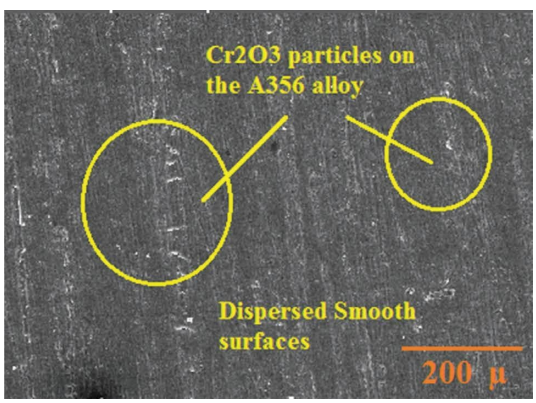

Figure 12: Maximum tensile attained specimens.

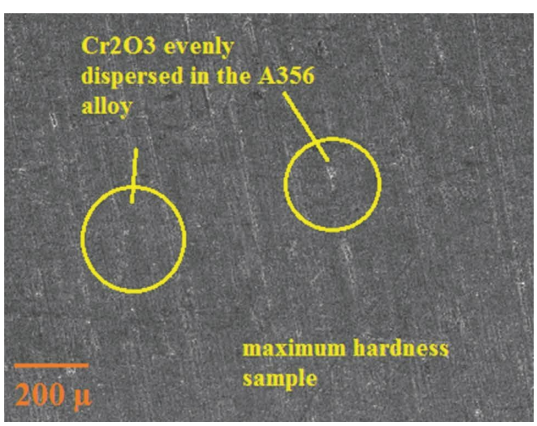

Figure 13: Maximum hardness attained specimens.

4. Conclusion

In this investigation, the A356 aluminium alloy and ceramic-based chromium oxide particles were successfully processed by the friction stir processing. The different FSP processing parameters such as tool spinning speed, tool pin sizes, and tool travel speed composes the better smooth finishing surfaces on the processed A356 alloy with reinforcing particles. Out of the different processing constraints, the maximum of tool spinning speed and minimum and maximum of tool pin sizes like 5 and 6 mm and minimum tool travel speed produces the better mechanical properties of tensile and micro hardness. The selected chromium oxide particles creates the sufficient heat while in the FSP and reduces the friction that would generate the more plasticized in the processed zones. The maximum tensile was attained at the processing parameters was 1500 rpm of spinning speed, 6 mm of tool pin sizes and 90 mm/min of tool travel speed. The maximum hardness was accomplished at the process parameters of 2000 rpm of spinning speed, 5 mm of tool pin sizes and 90 mm/min of tool travel speed, respectively. The SEM image reveals that the presence of chromium oxide particles dispersed evenly in the A356 aluminium matrix and it was the major causes for improving the tensile and hardness.

Data Availability

The data used to support the findings of this study are included in the article. Should further data or information be required, these are available from the corresponding author upon request.

Conflicts of Interest

The authors declare that there are no conflicts of interest regarding the publication of this paper.

Acknowledgments

The authors thank Villa College, Maldives, for providing characterization support to complete this research work.

References

[1] E. B. Moustafa, A. V. Mikhaylovskaya, M. A. Taha, and A. O. Mosleh, "Improvement of the microstructure and mechanical properties by hybridizing the surface of AA7075 by hexagonal boron nitride with carbide particles using the FSP process," *Journal of Materials Research and Technology*, vol. 17, pp. 1986–1999, 2022.

[2] M. Akbari, M. Ezzati, and P. Asadi, "Investigation of the effect of tool probe profile on reinforced particles distribution using experimental and CEL approaches," *International Journal of Lightweight Materials and Manufacture*, vol. 5, no. 2, pp. 213–223, 2022.

[3] M. Akbari, M. H. Shojaeefard, P. Asadi, and A. Khalkhali, "Hybrid multi-objective optimization of microstructural and mechanical properties of B4C/A356 composites fabricated by FSP using TOPSIS and modified NSGA-II," *Transactions of Nonferrous Metals Society of China*, vol. 27, no. 11, pp. 2317–2333, 2017.

[4] A. Sharma, H. Fujii, and J. Paul, "Influence of reinforcement incorporation approach on mechanical and tribological properties of AA6061- CNT nanocomposite fabricated via FSP," *Journal of Manufacturing Processes*, vol. 59, pp. 604–620, 2020.

[5] P. Vijayavel and V. Balasubramanian, "Effect of pin volume ratio on wear behaviour of friction stir processed LM25AA-5%SiCp metal matrix composites," *Alexandria Engineering Journal*, vol. 57, no. 4, pp. 2939–2950, 2018.

[6] C. Chanakyan and S. Sivasankar, "Parametric advancement of numerical model to predict the mechanical properties of friction stir processed AA5052," *International Journal of Rapid Manufacturing*, vol. 8, no. 1/2, p. 147, 2019.

[7] M. M. Z. Ahmed, M. M. El-Sayed Seleman, R. G. Eid, and M. F. Zawrah, "Production of AA1050/silica fume composite by bobbin tool-friction stir processing: microstructure, composition and mechanical properties," *CIRP Journal of Manufacturing Science and Technology*, vol. 38, pp. 801–812, 2022.

[8] A. Sharma, D. Narsimhachary, V. M. Sharma, B. Sahoo, and J. Paul, "Surface modification of Al6061-SiC surface composite through impregnation of graphene, graphite and carbon nanotubes via FSP: a tribological study," *Surface and Coatings Technology*, vol. 368, pp. 175–191, 2019.

[9] A. Zykova, A. Vorontsov, A. Chumaevskii et al., "Structural evolution of contact parts of the friction stir processing heat-resistant nickel alloy tool used for multi-pass processing of Ti6Al4V/(Cu+Al) system," *Wear*, vol. 488, Article ID 204138, 2022.

[10] A. K. Srivastava, N. K. Maurya, A. R. Dixit, S. P. Dwivedi, A. Saxena, and M. Maurya, "Experimental investigations of A359/Si3N4 surface composite produced by multi-pass friction stir processing," *Materials Chemistry and Physics*, vol. 257, Article ID 123717, 2021.

[11] D. A. P. Prabhakar, A. K. Shettigar, M. A. Herbert et al., "A comprehensive review of friction stir techniques in structural materials and alloys: challenges and trends," *Journal of Materials Research and Technology*, vol. 20, pp. 3025–3060, 2022.

[12] S. Baek, J. Song, H. C. Lee et al., "Robust bonding and microstructure behavior of aluminum/high-strength steel lap joints using resistance element welding process for lightweight vehicles: experimental and numerical investigation," *Materials Science and Engineering*, vol. 833, Article ID 142378, 2022.

[13] K. Jagathesh, M. P. Jenarthanan, P. D. Babu, and C. Chanakyan, "Analysis of factors influencing tensile strength in dissimilar welds of AA2024 and AA6061 produced by Friction Stir Welding (FSW)," *Australian Journal of Mechanical Engineering*, vol. 15, no. 1, pp. 19–26, 2017.

[14] B. Mirshekari, A. Zarei-Hanzaki, A. Barabi et al., "Optimizing the austenite stability in a ferritic lightweight steel through thermomechanical processing," *Materials Characterization*, vol. 166, Article ID 110367, 2020.

[15] C. Thiagarajan, T. Shaafi, and A. Muniappan, "Machinability studies on hybrid nano-SiC and nano-ZrO2 reinforced aluminium hybrid composite by wire-cut electrical discharge machining," *Materials Today: Proceedings*, 2021.

[16] Y. Mazaheri, R. Malmir, M. M. Jalilvand, M. Sheikhi, and A. Heidarpour, "Mechanical properties and tribological performance of A356/Cr3C2-NiCr surface composite developed by high-velocity oxy-fuel and post friction stir processing treatment," *Surfaces and Interfaces*, vol. 28, Article ID 101627, 2022.

[17] M. Orłowska, F. Pixner, A. Hütter, N. Enzinger, L. Olejnik, and M. Lewandowska, "Manufacturing of coarse and ultrafine-grained aluminum matrix composites reinforced with Al2O3 nanoparticles via friction stir processing," *Journal of Manufacturing Processes*, vol. 80, pp. 359–373, 2022.

[18] S. Sivasankar et al., "Parametric studies in friction stir welding on al-mg alloy with (Hchcr) tool by taguchi based desirability function analysis (dfa)," *Journal of Ceramic Processing Research*, vol. 21, no. 6, 2020.

[19] A. H. Maamoun, S. C. Veldhuis, and M. Elbestawi, "Friction stir processing of AlSi10Mg parts produced by selective laser melting," *Journal of Materials Processing Technology*, vol. 263, pp. 308–320, 2019.

[20] M. M. El-Sayed, A. Y. Shash, M. Abd-Rabou, and M. G. ElSherbiny, "Welding and processing of metallic materials by using friction stir technique: a review," *Journal of Advanced Joining Processes*, vol. 3, Article ID 100059, 2021.

[21] N. A. Liyakat and D. Veeman, "Improvement of mechanical and microstructural properties of AA 5052-H32 TIG weldment using friction stir processing approach," *Journal of Materials Research and Technology*, vol. 19, pp. 332–344, 2022.

[22] D. Harwani, V. Badheka, V. Patel, W. Li, and J. Andersson, "Developing superplasticity in magnesium alloys with the help of friction stir processing and its variants – a review," *Journal of Materials Research and Technology*, vol. 12, pp. 2055–2075, 2021.

[23] L. F. Ali, N. Kuppuswamy, R. Soundararajan, K. R. Ramkumar, and S. Sivasankaran, "Microstructural evolutions and mechanical properties enhancement of AA 6063 alloy reinforced with Tungsten (W) nanoparticles processed by friction stir processing," *Materials Characterization*, vol. 172, Article ID 110903, 2021.

[24] H. Kumar, R. Prasad, P. Kumar, S. P. Tewari, and J. K. Singh, "Mechanical and tribological characterization of industrial wastes reinforced aluminum alloy composites fabricated via friction stir processing," *Journal of Alloys and Compounds*, vol. 831, Article ID 154832, 2020.

[25] M. Ebrahimi and M. A. Par, "Twenty-year uninterrupted endeavor of friction stir processing by focusing on copper and its alloys," *Journal of Alloys and Compounds*, vol. 781, pp. 1074–1090, 2019.

[26] X. H. Zeng, P. Xue, L. H. Wu, D. R. Ni, B. L. Xiao, and Z. Y. Ma, "Achieving an ultra-high strength in a low alloyed Al alloy via a special structural design," *Materials Science and Engineering*, vol. 755, pp. 28–36, 2019.

[27] M. Zhou, Z. Zeng, C. Cheng et al., "Effect of the processing route on the microstructure and mechanical behavior of superlight Mg-9Li-1 Zn alloy via friction stir processing," *Journal of Magnesium and Alloys*, vol. 10, no. 11, pp. 3064–3081, 2022.

[28] S. Suresh, E. Natarajan, R. Shanmugam, K. Venkatesan, N. Saravanakumar, and A. AntoDilip, "Strategized friction stir welded AA6061-T6/SiC composite lap joint suitable for sheet

metal applications," *Journal of Materials Research and Technology*, vol. 21, pp. 30–39, 2022.

[29] M. Mondal, H. Das, S. T. Hong, B. S. Jeong, and H. N. Han, "Local enhancement of the material properties of aluminium sheets by a combination of additive manufacturing and friction stir processing," *Corporate Insolvency Resolution Process Annals*, vol. 68, no. 1, pp. 289–292, 2019.

[30] X. C. Luo, D. T. Zhang, G. H. Cao, C. Qiu, and D. L. Chen, "High-temperature tensile behavior of AZ61 magnesium plate prepared by multi-pass friction stir processing," *Materials Science and Engineering*, vol. 759, pp. 234–240, 2019.

[31] S. Rajkumar, K. Mageshkumar, K. Arul, S. Ravi, T. Maridurai, and R. Subbiah, "Effect of welding speed on the mechanical properties of AA6061 Al alloy joined by friction stir welding," *Materials Today: Proceedings*, vol. 59, pp. 1544–1549, 2022.

[32] J. Stephen Leon et al., "Heat index based optimisation of primary process parameters in friction stir welding on light weight materials," *Advances in Materials Science and Engineering*, vol. 2022, Article ID 2494750, 9 pages, 2022.

[33] L. Karthick, R. Rathinam, S. A. Kalam et al., "Influence of nano-/microfiller addition on mechanical and morphological performance of kenaf/glass fibre-reinforced hybrid composites," *Journal of Nanomaterials*, vol. 2022, Article ID 9778224, 10 pages, 2022.

[34] L. Karthick, S. Sivakumar, A. Sasikumar, A. Prabhu, J. Senthil Kumar, and L. Vadivukarasi, "A comparison and analysis of mechanical properties of glass fiber and banana fiber composite," *Materials Today: Proceedings*, vol. 52, no. 3, pp. 398–402, 2022.

[35] L. Karthick, J. Stephen leon, R. ravi, J. Michel, N. Mallireddy, and L. Vadivukarasi, "Modelling and analysis of an EN8 crankshaft in comparison with AISI 4130 crankshaft material," *Materials Today: Proceedings*, vol. 52, no. 3, pp. 1036–1040, 2022.

[36] L. Karthick, N. Mallireddy, J. Yogaraja, S. Sivakumar, and A. Sasikumar, "Modelling and Analysis of an EN8 crankshaft material in comparison with Forged steel crankshaft," *Materials Today: Proceedings*, vol. 47, no. 17, pp. 6168–6172, 2021.

[37] Y. Sesharao, T. Sathish, K. Palani et al., "Optimization on operation parameters in reinforced metal matrix of AA6066 composite with HSS and Cu," *Advances in Materials Science and Engineering*, vol. 2021, Article ID 1609769, 12 pages, 2021.

[38] C. Chanakyan, S. Sivasankar, M. Meignanamoorthy et al., "Optimization of FSP process parameters on AA5052 employing the S/N ratio and ANOVA method," *Advances in Materials Science and Engineering*, vol. 2021, Article ID 6450251, 15 pages, 2021.